Full Length Article

Oxygen accumulation on metal surfaces investigated by XPS, AES and LEIS, an issue for sputter depth profiling under UHV conditions

R. Steinberger [a],[*], C.E. Celedón [b],[c], B. Bruckner [b], D. Roth [b], J. Duchoslav [a], M. Arndt [d], P. Kürnsteiner [a], T. Steck [d], J. Faderl [d], C.K. Riener [d], G. Angeli [d], P. Bauer [b], D. Stifter [a]

[a] Center for Surface and Nanoanalytics, Johannes Kepler University Linz, Altenberger Straße 69, 4040 Linz, Austria
[b] Institut für Experimentalphysik, Abteilung für Atom- und Oberflächenphysik, Johannes Kepler University Linz, Altenberger Straße 69, 4040 Linz, Austria
[c] Departamento de Física, Universidad Técnica Federico Santa María, Valaparaíso, Casilla 110-V, Chile
[d] voestalpine Stahl GmbH, voestalpine-Straße 3, 4031 Linz, Austria

ABSTRACT

Depth profiling using surface sensitive analysis methods in combination with sputter ion etching is a common procedure for thorough material investigations, where clean surfaces free of any contamination are essential. Hence, surface analytic studies are mostly performed under ultra-high vacuum (UHV) conditions, but the cleanness of such UHV environments is usually overrated. Consequently, the current study highlights the in principle known impact of the residual gas on metal surfaces (Fe, Mg, Al, Cr and Zn) for various surface analytics methods, like X-ray photoelectron spectroscopy (XPS), Auger electron spectroscopy (AES) and low-energy ion scattering (LEIS). The investigations with modern, state-of-the-art equipment showed different behaviors for the metal surfaces in UHV during acquisition: (i) no impact for Zn, even after long time, (ii) solely adsorption of oxygen for Fe, slight and slow changes for Cr and (iii) adsorption accompanied by oxide formation for Al and Mg. The efficiency of different counter measures was tested and the acquired knowledge was finally used for ZnMgAl coated steel to obtain accurate depth profiles, which exhibited before serious artifacts when data acquisition was performed in an inconsiderate way.

© 2017 Elsevier B.V. All rights reserved.

1. Introduction

For a detailed characterization of materials and sample structures depth profiling with highly surface sensitive methods in combination with sputter ion etching is commonly used. In this case clean surfaces, which also have to stay free of contaminations during the entire experiment, are calling for ultra-high vacuum (UHV) equipment. Although the pressure of the residual gas is very low under common UHV conditions the surfaces are never kept permanently clean [1–4], which is especially challenging in the context of surface analysis or depth profiling of metals and their oxides. In this context basic oxidation studies shall be mentioned, where the formation of iron oxides on metallic iron due to exposure to low oxygen pressures was already investigated in depth, *e.g.* [5–10]. Nevertheless, the number of studies on iron or steel dealing with the influence of the residual gas within UHV chambers is quite low, *e.g.* [11]. For other metals such as Al, Mg and Cr a large number of studies about defined oxidation, including the initial stages and determination of sticking coefficients, as well as work function changes due to chemisorption of water and oxygen are available [12–19]. However, also here the impact of the residual gas was never put into the main focus of these investigations. Only Kasupke et al. [20] provided insight into the effect of contaminations by the residual gas on cleaved silicon and Ramsey et al. [21] briefly reported on exo-electron emission from abraded metal surfaces under UHV conditions.

The issue of contaminations arising from residual gas has been in principle known for decades and was already considered for depth profiling with abrasive techniques [1,2,11]. However, there is a lack of studies using modern equipment, like state-of-the-art X-ray photoelectron spectroscopy (XPS) machines with, *e.g.*, dual flood guns for sophisticated charge neutralization, and using differ-

* Corresponding author.
E-mail addresses: roland.steinberger@jku.at, r_steinberger@gmx.at
(R. Steinberger), carlos.celedon@usm.cl (C.E. Celedón), barbara.bruckner@jku.at
(B. Bruckner), dietmar.roth@jku.at (D. Roth), jiri.duchoslav@jku.at
(J. Duchoslav), martin.arndt@voestalpine.com (M. Arndt), p.kuernsteiner@mpie.de
(P. Kürnsteiner), thomas.steck@voestalpine.com (T. Steck),
josef.faderl@voestalpine.com (J. Faderl), christiankarl.riener@voestalpine.com
(C.K. Riener), gerhard.angeli@voestalpine.com (G. Angeli), peter.bauer@jku.at
(P. Bauer), david.stifter@jku.at (D. Stifter).

ent acquisition concepts as in the afore mentioned older studies; as an example, mostly no continuous sputtering can normally be performed during data acquisition, since the time needed to record all essential high-resolution spectra would lead on complex materials to an intolerable loss of depth resolution. Hence, in the current study three surface sensitive methods, namely XPS, Auger electron spectroscopy (AES) and low-energy ion scattering (LEIS), which exhibits an even higher surface sensitivity [22], were considered and compared with the aim to clarify the consequences of oxygen uptake in depth profiling studies and to test counter measures. The focus is finally put on a reliable analysis of ZnMgAl coatings, which were developed as a modern and efficient concept for corrosion protection of steel [23], by carefully taking the arising artifacts into account.

2. Material and methods

2.1. Sample preparation

Depth profiles of ZnMgAl coated standard low-carbon steel obtained from voestalpine Stahl GmbH were recorded. The coatings were fabricated by hot-dip galvanizing and consist of 96 wt.% Zn, 2.5 wt.% Al and 1.5 wt.% Mg with a layer thickness of approximately 7 μm. Also samples of the bare steel substrate were used in this study. In addition, a piece of high-purity iron (~99.8%) obtained from voestalpine was considered for further investigations. For angle resolved XPS measurements (ARXPS) the steel and iron samples were polished using diamond pastes down to a particle size of 1 μm. A standard cleaning procedure by ultrasonication in tetrahydrofuran, isopropanol and finally ethanol, as already described elsewhere [23], was carried out for the metal substrates. A magnesium rod of high purity (Sigma-Aldrich, ≥99.9% metal basis) was cut and polished to obtain a smooth metallic Mg surface; only ethanol was used in the ultrasonic bath for sample cleaning. Furthermore, a piece of aluminum foil was taken for testing a metallic Al surface. The surface of a block of Cr was polished and subsequently exposed to several cycles of ultrasonication in isopropanol and ethanol. Finally, a sample was taken from a high-purity zinc foil (Sigma-Aldrich, ≥99.99% metal basis). Prior to the measurements, all these metal surfaces were *in situ* sputter cleaned.

2.2. Instrumentation

The XPS measurements were performed on a Theta Probe (ThermoFisher, UK) with the Avantage software package for the control of the instrument, for data acquisition and evaluation. For excitation, a monochromated Al-K$_\alpha$ X-ray source (1486.7 eV, 15 kV, 3 mA, 45 W, spot size of 200 μm) was chosen. The hemispherical electron energy analyzer was set for the acquisition of high-resolution spectra to a pass energy of 50 eV and an energy channel step width of 0.1 eV. The associated multi-channel detection system (112 energy channels and 96 angle channels) enables non-destructive depth profiling of the topmost surface layers by ARXPS (take-off angle between 20° and 80° with respect to the surface normal). For charge neutralization the system is equipped with a dual flood gun which provides low-energy electrons (~2 eV) as well as Ar$^+$ ions with low kinetic energy (~20 eV). The Theta Probe, evacuated by turbomolecular pumps and supported by a titanium sublimation pump, exhibits a base pressure in the low 10^{-9} to mid 10^{-10} mbar range and an operation pressure in the lower half of the 10^{-7} mbar range during sputtering and when the flood gun is on. The Ar$^+$ ion gun was operated with an acceleration voltage of 3 keV and an ion current of 1 μA with a size of the sputter crater of 2 × 2 mm on the sample. The etch cycles for the ZnMgAl sample were 480 s for each of the first 25 steps of sputtering, followed by 10 steps of 2400 s each, and

finally 3 steps with a duration of 18000 s each. Data evaluation was started with the elimination of the peak backgrounds by applying Shirley background subtraction [24], subsequently the peak areas were normalized using Scofield sensitivity factors [25] to obtain the elemental composition.

For complementary investigations a scanning Auger electron spectrometer from JEOL (JAMP 9500F) was used. This UHV setup (base pressure ~5 × 10^{-10} mbar, with a sputter ion pump and a titanium sublimation pump) is based on a scanning electron microscope (SEM) with a Schottky field emitter, which is additionally equipped with an electron analyzer containing a detection unit with 7 channeltrons. High-resolution measurements in the range of 0 up to 2500 eV with a spatial resolution down to 8 nm can be carried out. An Ar$^+$ ion gun with a selectable ion energy from 0.5 up to 3 keV is mounted for the purpose of surface cleaning, to acquire depth profiles and for charge neutralization by choosing ions with low kinetic energy (minimum 10 eV).

The LEIS measurements were performed on an ESA-LEIS (electrostatic analyzer low-energy ion scattering) setup with a base pressure lower than 5 × 10^{-10} mbar using a turbomolecular pump, a sputter ion pump, a titanium sublimation pump and a cold trap. A beam of He$^+$ ions with kinetic energies selectable in the range of 0.3 up to 5 keV with a primary beam current ranging from 0.05 to 1 nA is directed perpendicular towards the sample surface. Backscattered He$^+$ ions with a scattering angle of 136° enter a cylindrical mirror analyzer and are detected by a set of micro channel plates. When applying Ar instead of He gas sputter cleaning can be performed. For an analysis of the sample composition the peak areas of the surface peaks were evaluated, after subtraction of the background due to reionization in deeper layers and by using scattering cross sections derived from the ZBL (Ziegler, Biersack, Littmark) potential [26].

2.3. Measurement procedure

Photoelectron levels (C1s, O1s, Zn2p, Cr2p, Fe2p, Mg2p and Al2p) and – when appropriate – the associated Auger transitions (ZnL$_{23}$M$_{45}$M$_{45}$ and MgKL$_{23}$L$_{23}$) were recorded by XPS in the center position of the sputter craters, which either were arising from the sputter cleaning steps or by depth profiling. The measurements which focused solely on the oxygen uptake were performed in a continuous way by iteratively acquiring the spectra of interest. The peak of adventitious carbon was not used for charge shift correction because in most cases it was of very low intensity or even absent. Furthermore, the issue of differential charging [27] might cause serious inconsistencies; especially the dynamic changes of the surface composition and consequently different prevailing conditions of the conductivity due to oxygen adsorption and potentially following oxidation can strongly influence the obtained peak positions. Hence, instead of using absolute binding energy values for the data evaluation relative peak separations, unique and special peak features such as shake-up satellites and/or multiplet splitting, and the modified Auger parameter (MAP, a simple method to distinguish between different chemical states) [28] were taken into account. For fitting of the recorded data Gaussian-Lorentzian shaped peaks as well as specific reference spectra from an own data base [27] were used. When assuming a uniform oxide layer on top of a metal the layer thickness can be estimated by comparing the photoelectron peak intensities of the oxidic and the metallic part [29]. Furthermore, the inelastic mean free paths (IMFPs), the electron take-off angle, and the volume densities are needed for the calculation. The required IMFPs for Al2p photoelectrons within Al metal (26 Å) and Al$_2$O$_3$ (28 Å) were deduced from [30,31]. In case of ARXPS the take-off angle is well-defined, for the standard acquisition mode a mean value of 50° – relative to the surface normal – was chosen.
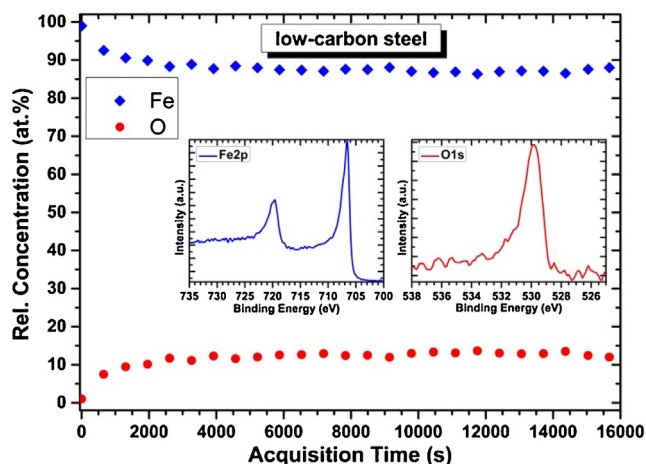
Fig. 1. Relative concentration plot of iron and oxygen obtained from sputter-cleaned low-carbon steel showing an uptake of oxygen over acquisition time. The high-resolution spectra of Fe2p and O1s of the last measurement step are shown in the inset.

The ESA-LEIS measurements were performed on the polished steel sample, using Ar^+ ion bombardment with 3 keV and 10–15 nA as preliminary cleaning step. The threshold energy for reionization processes is for iron 900 eV, below Auger neutralization dominates. For the acquisition of full-energy range spectra a kinetic energy of 2 keV was chosen. At this energy, resonant processes (reionization and resonant neutralization) contribute considerably to charge exchange, which facilitates surface composition analysis due to the absence of matrix effects [32]. The data evaluation comprises a quantitative evaluation of the ion yields for Fe and O after surface cleaning and for various experimental times.

3. Results and discussion

3.1. XPS, LEIS and AES investigations on metallic Fe surfaces

The main motivation for the current study is related to observations made in routinely recorded XPS sputter depth profiles from various Zn-based coatings (Zn, ZnCr, ZnMgAl) on low-carbon steel sheets. In detail, at the interface between the coating and the steel an increase of oxygen was always observed until a steady state of approximately 90 at.% of iron and 10 at.% of oxygen was reached within the substrate region, where no noteworthy amounts of oxygen should be present. In the following, various investigations on the surface of chemically and sputter-cleaned sheets of the bare low-carbon steel were performed considering different surface sensitive analysis methods. Complementary data of three autonomous UHV setups with different pumping systems could be obtained in this way. At first, data from iterative XPS measurements of the Fe2p and O1s signals of an initially sputter cleaned steel surface is shown in Fig. 1.

It is evident that the original concentration of 100 at.% metallic iron is decreased by an enrichment of oxygen over time with final concentration values of approximately 88 at.% Fe and 12 at.% O. Although the O1s level taken from the last measurement is clearly indicative for the presence of oxygen, there is no evidence for oxidized iron, as proven by the corresponding Fe2p spectrum. In order to identify the source of oxygen systematic experiments – considering (i) migration processes of contaminations from the regions next to the sputter crater into the analysis region, (ii) reactions induced by X-ray irradiation, electrons or Ar^+ ions (originating from the dual flood gun), (iii) impurities in the gas system of the dual flood gun/ion gun or a (iv) potential UHV leak of the chamber –

were performed leading to the conclusion that the sole origin of the accumulated oxygen on the surface is related to the residual gas inside the UHV chamber, which generally contains for UHV setups evacuated by turbomolecular pumps H_2, H_2O, CO, CO_2 and O_2 [33–36]. Also our own investigations of the residual gas in an attached preparation chamber of the XPS by using a quadrupole mass spectrometer showed no unusual composition, but quantitatively this depends besides the type of pumps on many factors like bake-out parameters, getter objects, cold traps and cooling stages, frequency and procedure of sample transfers, and history of measured samples.

In the case of the high-purity iron sample the final concentrations and the accumulation kinetics were found to be similar as observed for the low-carbon steel in the previous experiments. Furthermore, ARXPS data were acquired after the steady state concentration of oxygen had been reached. All of the Fe2p spectra obtained from the different angles (related to different average depths) perfectly matched the one of a metallic iron reference. Neither the bulk sensitive signal, nor the surface sensitive spectra revealed any traces of iron in a higher oxidation state showing that the electronic structure of iron is not recognizably influenced by the oxygen accumulation in our experimental time frame, *i.e.*, an oxygen containing species is simply adsorbed with no formation of iron oxide. In this context, a detailed description on the initial stages of oxidation can be found in some publications, *e.g.*, [7–10]. For the sake of completeness, it should be noted that XPS standard quantifications, as routinely performed by the community for the overwhelming part of measurements, are based on assuming a homogeneous distribution of all elements within the information depth of XPS. In the current case of iron and steel the found oxygen is adsorbed on top, whereas the distance between an adsorbed atom and the substrate atom can be estimated by the sum of their van der Waals radii [37]. Assuming a monolayer thickness with the double of the van der Waals radius of oxygen the fractional surface coverage can be calculated according to [38]. With inelastic mean free paths of $Fe2p_{3/2}$ and O1s photoelectrons in the oxygen overlayer taken from [39] or by using the attenuation lengths determined according to [40] coverage values of ~90% or slightly more than 100%, respectively, were obtained. Taking these results and the lack of knowledge on the exact nature of the adsorbent into account the surface coverage can be considered equaling a full monolayer.

For the investigation of Zn-based coatings on steel cooling is one of the few sufficiently well working counter measures to slow down and decrease X-ray induced radiation damage of unstable corrosion products or their degradation due to monoatomic ion bombardment, as shown by us in [41–43]. Since the sticking coefficient for the impinging gas particles depends on the sample temperature a freshly cleaned low-carbon steel sample was cooled and kept in a long-term experiment at −120 °C. From the obtained data it became evident that the cooled sample surface gathers more oxygen or oxygen containing components from the residual gas and that the oxygen concentration clearly surpassed the value of ~12 at.% from the experiments at room temperature. At these higher concentrations oxidation of the iron surface was finally visible in the Fe2p spectra (not shown).

For comparison ESA-LEIS was also performed on a sample of polished and *in situ* sputter-cleaned low-carbon steel. This technique is known to be extremely surface sensitive, since for noble gas ions the ion fraction P^+ is very low for ions being backscattered from subsurface layers of the target [44–46]. Full-energy spectra were iteratively recorded with a period of 5 min, and are shown together with the evolution of the deduced ion yields for iron and oxygen in Fig. 2a).

The freshly cleaned surface is free of contaminations and initially no oxygen could be detected. With increasing time an increase of the oxygen peak is also in this setup evident (the LEIS spectra are
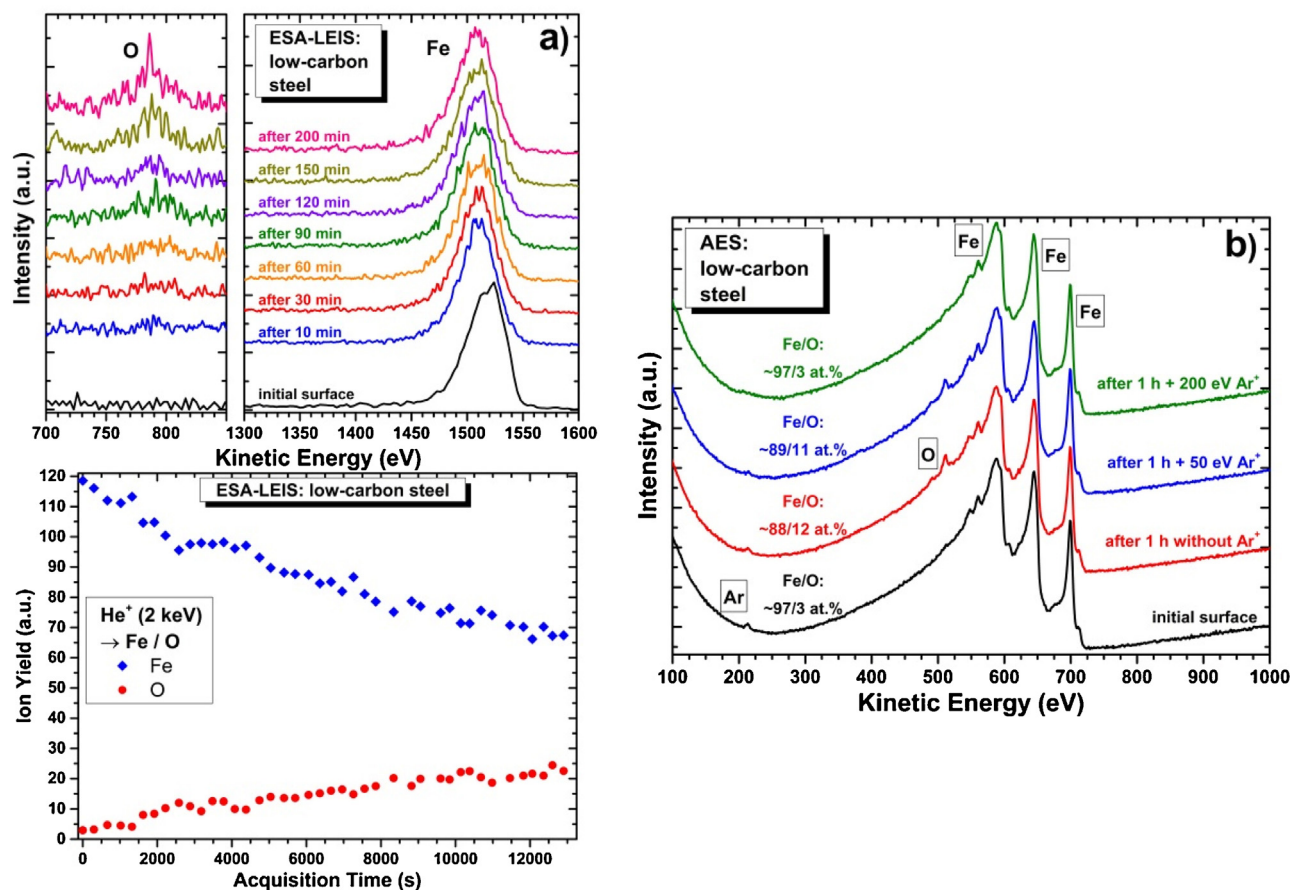
Fig. 2. **a**) ESA-LEIS measurements with He$^+$ ions of 2 keV primary energy on a polished and sputter-cleaned low-carbon steel sample. The energy spectrum shows the intensity of the ions backscattered from the Fe and O atoms for different exposure times to the residual gas; the corresponding evolution of Fe and O ion yields is depicted below. **b**) Auger electron data from an initially clean low-carbon steel surface, with a spectrum recorded after a waiting time of one hour, and two spectra after waiting for an hour with continuous Ar$^+$ ion bombardment of low kinetic energy with 50 eV and 200 eV, respectively.

normalized with respect to the Fe signal). The apparent different peak position of the initial Fe signal might be related to a change in the inelastic losses due to the adsorbate-metal interaction. From the full-range spectra the ion yields for He$^+$ scattered from Fe and O, respectively, were evaluated and plotted as a function of acquisition time as given in the bottom plot of Fig. 2a), showing a rapid decrease for the yield from Fe atoms.

As a third method Auger electron spectroscopy, performed again in a separate, autonomous UHV system (with sputter ion pump), was used on the low-carbon steel material. A chemically cleaned sample was *in situ* sputter-cleaned by Ar$^+$ ions before a fast data acquisition step followed. The spectrum shows a more or less oxygen free surface, however due to the finite signal-to-noise ratio the quantification algorithm yielded a ratio of 97:3 at.% for Fe to O (Fig. 2b)). Afterwards the sample was kept in place for an hour with the electron beam being blocked and finally measured again. The quantification gives an Fe to O concentration of 87.7 at.% vs. 12.3 at.%, *i.e.*, a similar amount of oxygen absorbed on the steel substrate as found in the XPS experiments. This fact together with the lack of carbon in the XPS spectra hints on a quite insignificant contribution of potential contaminations originated by bearing oil used in turbomolecular pumps, as the ones attached to the XPS system. After sputter-cleaning this AES experiment was repeated two times, with a sputter cleaning step always before, once with bombarding the sample surface during the waiting time with Ar$^+$ ions of 50 eV kinetic energy and once with 200 eV ions from the ion gun (charge neutralization mode). The data as shown in Fig. 2b) revealed a ratio Fe:O of 89:11 at.% and 96.6:3.4 at.%, respectively,

which points out that ions of 50 eV are not sufficient while ions of 200 eV are suited to totally hinder oxygen uptake. A similar concept, namely a continuous sputter bombardment during Auger spectra acquisition using Ar$^+$ ions of 3 keV, was already applied for depth profiling of stainless steel [11]. However, a gentler mode should significantly decrease the sputter yield, which is essential to obtain a reasonable depth resolution. This is of high importance when the number of required high-resolution scans increases the acquisition time dramatically, as it is the case for complex material systems involving many elements. Nevertheless, it has to be considered that even for these low kinetic ion energies serious chemical changes/damage may be induced [42,43].

3.2. XPS investigations on metallic Mg, Al, Cr and Zn surfaces

In the following, different *in situ* sputter-cleaned metal surfaces were investigated by XPS which are relevant for, *e.g.*, Zn-based anti-corrosion coatings (Zn, ZnCr, ZnMgAl) [23,47] or metal alloys [12]. In contrast to other surface studies [12–15,19,48], here the main focus is put on the impact of the residual gas, as shown in Fig. 3a)–d) for Mg, Al, Cr and Zn. Both, the individual oxygen concentration as a function over time and the evolution of the Mg2p, Al2p, Cr2p$_{3/2}$, ZnL$_{23}$M$_{45}$M$_{45}$ and O1s levels are presented.

The oxygen uptake of the Mg surface is in comparison to the experiments on the Fe surface substantially increased with the signals heading towards a final concentration of about 61 at.% Mg and 39 at.% O (Fig. 3 a)). Changes in the spectra of Mg2p are equally evident, with the formation of mainly MgO and a decrease of the
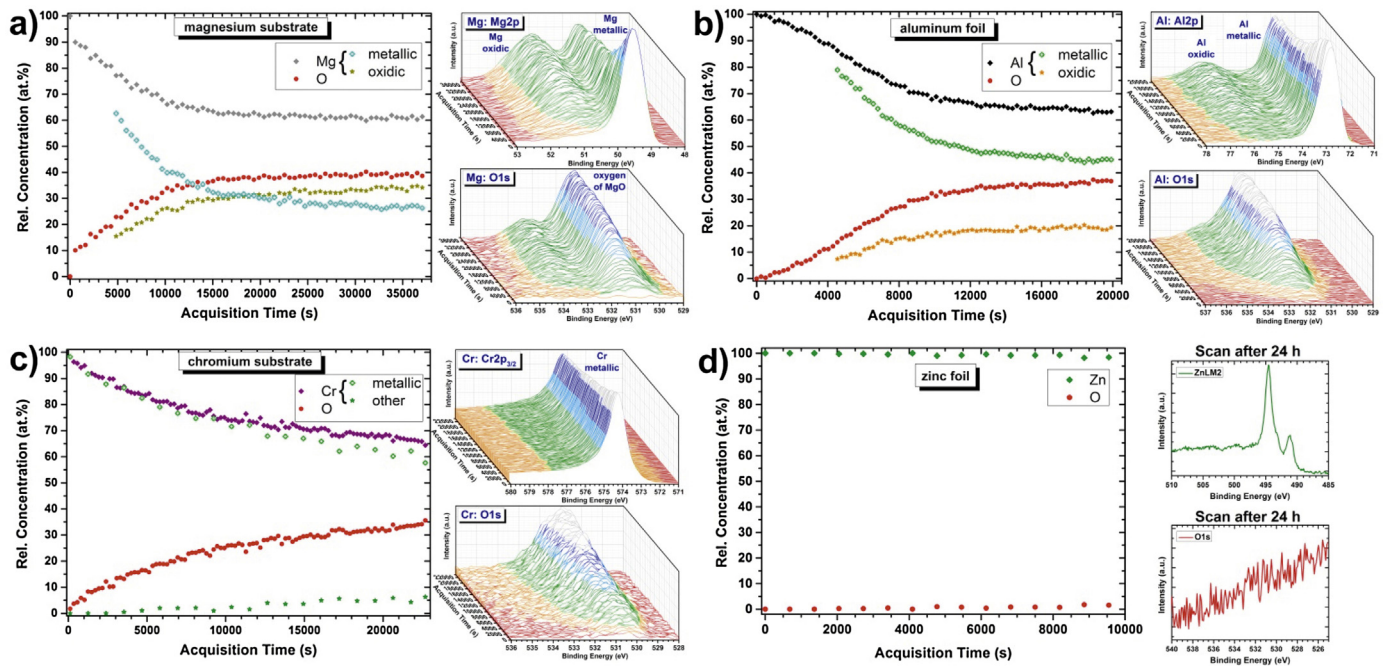
Fig. 3. The relative concentration plots of **a**) Mg, **b**) Al, **c**) Cr, **d**) Zn with respect to O from initially sputter-cleaned metallic surfaces are shown as a function of acquisition time, including a differentiation between metallic and oxidic species. In addition, the high-resolution spectra of Mg2p, Al2p, Cr2p$_{3/2}$, ZnL$_{23}$M$_{45}$M$_{45}$ and O1s are given as a function of exposure time, which are indicative for changes in the electronic structure of the surface atoms (except for zinc).

content of the metallic species. The spectra of the O1s level reveal next to the oxygen being attributed to MgO an increasing peak at higher binding energy side. This one may belong to an adsorbed type [49,50], *e.g.*, in form of accumulated water or more likely according to [14,51] to oxygen in a "defective" chemical environment. The Mg2p spectra were fitted for acquisition times exceeding 5000 s (before the peak intensities were too low for accurate fits) with an oxidic and a metallic contribution by using a reference of metallic magnesium and a Gaussian-Lorentzian shaped peak representing the oxidic Mg type.

Also for the Al sample an increase of the oxygen signal, and simultaneously, a decrease of the aluminum signal over time are evident (Fig. 3b)). The evolution of the oxygen signal does not follow a simple exponential behavior as observed before on Fe and Mg. Furthermore, the spectra of Al2p and O1s levels clearly indicate the growth of aluminum oxide. In order to roughly quantify the transformation from metallic to oxidic Al the Al2p spectra were fitted for acquisition times longer than 4500 s with reference spectra. Due to a slight excess of oxygen with respect to the expected stoichiometry of Al$_2$O$_3$ and due to a recognizable small shoulder in the O1s spectra at the high binding energy side, the presence of a simply adsorbed oxygen species is indicated. More details on the fundamental processes of aluminum oxidation can also be found in, *e.g.*, [12,19,48]. In addition, non-destructive depth profiling was performed by ARXPS when equilibrium conditions of the aluminum and oxygen concentrations were reached. The deeper layers showed a predominating presence of metallic aluminum while the oxygen signal increased towards the surface regions. The O1s spectra could be fitted with a part belonging to aluminum oxide and another one being related to a second, different type. An evaluation according to [29] of the Al2p peak intensity ratios of the oxidic to the metallic contribution for all of the recorded angles gave an average layer thickness of 4.6 ± 0.4 Å, which is in good agreement to a thickness of 5 Å as obtained from a calculation based on the final spectrum of Fig. 3b). Further data evaluation, by assuming a two overlayer structure on the metallic bulk indicates that the oxide layer is covered itself by the oxygen contribution of the sec-

ond type. An average layer thickness of ∼1 Å was obtained from the angle resolved data for this topmost layer. According to literature [12,19] this contribution can be related to adsorbed water or OH species, also the presence of less coordinated and incorporated oxygen is possible.

In the case of Cr, the metallic surface is as well subjected to an increasing O1s signal while the Cr2p$_{3/2}$ signal decreases over time (Fig. 3c)). The uptake of oxygen follows, like for Fe and Mg, an exponential behavior. The Cr2p$_{3/2}$ spectra reveal slight indications for chemical changes over time. In detail, at higher binding energy side of the metallic Cr peak a shoulder grows, which is too small for reliable fitting with reference spectra. However, the evolution from metallic species into another Cr type was evaluated by taking the peak areas, as shown in the relative concentration plot. The obtained data indicate that most of the oxygen is simply adsorbed. Further detailed information on the initial stages of oxidation of Cr, proposed as models, can be found in [10,13,16–18].

In contrast to the above studied metals, the spectra obtained from a Zn surface revealed no remarkable oxygen uptake, as shown in the relative concentration plot in Fig. 3d). Even after a period of ∼24 h, the O1s and ZnL$_{23}$M$_{45}$M$_{45}$ levels are devoid of any indication for an increase of oxygen. This circumstance is most probably related to sublimation of zinc from the surface induced by its higher vapor pressure, as compared to the other investigated metals. Furthermore, different studies report on slow adsorption processes of molecular oxygen and the necessity for larger exposures to saturate the surface [52–54].

3.3. XPS depth profiles on ZnMgAl coated steel

In order to obtain insights on the impact of oxygen accumulation for common analysis tasks in XPS depth profiling by Ar$^+$ ion sputtering, a ZnMgAl coated steel sample was investigated. The coating exhibits a non-uniform lateral composition, which is related to enclosed Zn-rich dendrites and eutectic phases including Zn, MgZn$_2$ and Al [23,55]. Hence, to exclude the influence of lateral inhomogeneities, all spectra were acquired at exactly the same position for
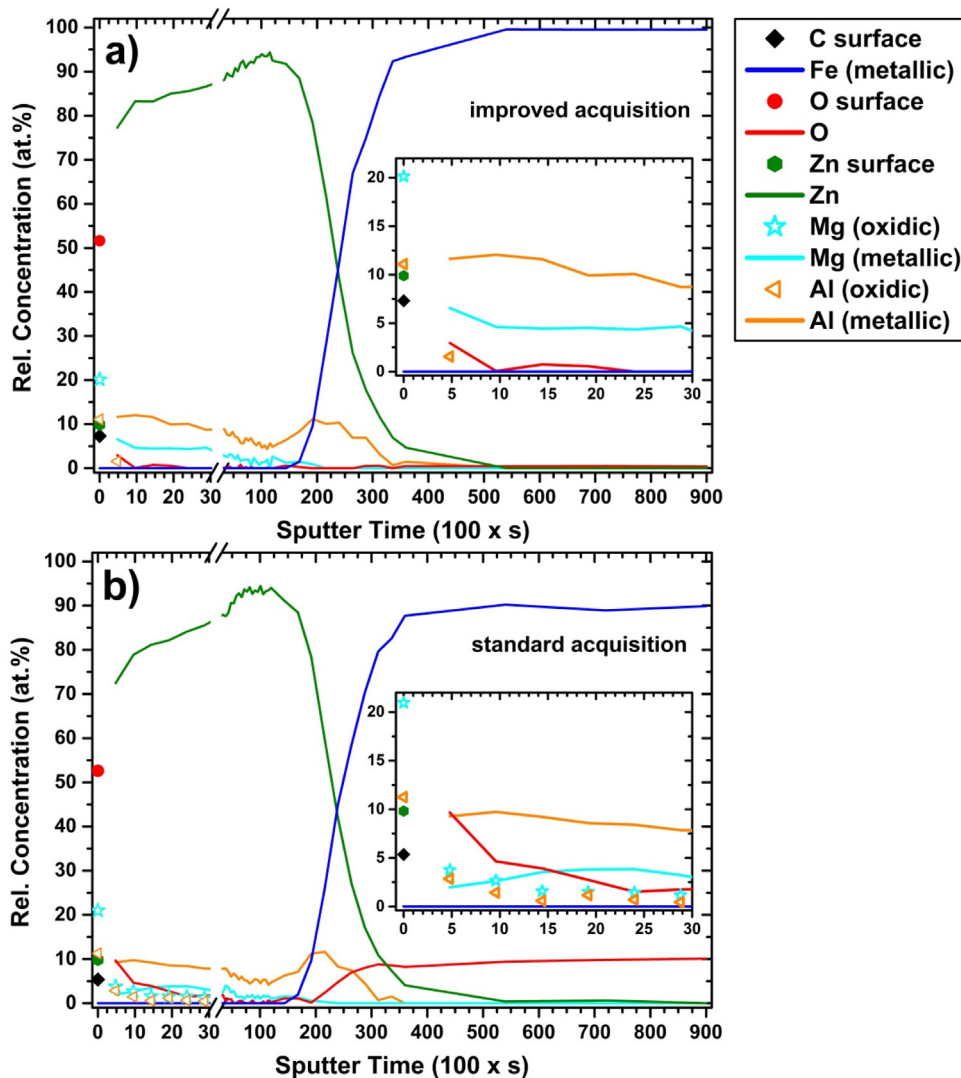
Fig. 4. Comparison of sputter depth profiles: chemical composition as a function of the sputter time for a ZnMgAl coated steel obtained from an identical measurement position reveals measurement artifacts caused by oxygen uptake from the residual gas. The standard profile **b**) results from a regular data acquisition procedure as it would be applied for a not fully known sample composition, including longer measurement times for better chemical peak fitting. The improved profile **a**) was obtained from a well-considered sequence of spectra acquisition and minimizing measurement time.

both presented experiments. The spectra of the profile shown in Fig. 4a) were always recorded at first with an absolute minimum of acquisition time. This profile is much more accurate regarding the real depth composition (sputter technique based artifacts like preferential sputtering, atomic mixing or partial chemical degradation may still persist [56]), also because of a well-considered sequence of spectra acquisition with optimized parameters; O1s level at first, immediately followed by the levels being essential for the characterization and quantification of the oxidation states of Al and Mg, then Fe2p, and finally, the levels for Zn and carbon. This optimization, especially shortening the acquisition time and the selection of the relevant elements and their specific Auger and photoelectron peaks, can only be reasonably fulfilled when the sample structure and elemental composition is not totally unknown. The spectra for the second profile shown in Fig. 4b) were recorded immediately afterwards in a standard way with longer acquisition times for a better signal-to-noise ratio, as it might be done for a not fully known material composition, for more reliable peak fitting to obtain chemical information and little knowledge about a potential oxygen accumulation. The time spent for the spectra acquisition for the first profile plays in this second experiment the role of potential mea-

surements of additional Auger and photoelectron levels which are essential for, *e.g.*, coatings exposed to various surface treatments and corrosive atmospheres, involving additional elements like Cl, S, P or Na.

As seen in Fig. 4, the surface composition is found to be identical, besides a minimal drop of the carbon amount for the second profile caused by the longer exposure time to X-rays and dual flood gun. Also the Zn signals in both profiles, revealing on top oxidic and metallic species and in the following solely metallic Zn before vanishing, does not show any peculiarities over the whole depth range. The carbon signals totally vanished in both profiles after the first sputter cycle and also the evolution of the Al signal shows in both cases a maximum at the interface, which would correspond to an Al-Fe inhibition layer [57]. However, when comparing the evolution of Al and Mg for the first sputter cycles indeed a number of significant differences is evident. Fig. 4a) shows that the oxidic Mg on the surface is totally removed by the first sputter cycle, followed by metallic Mg. This behavior is similar for Al, which is on top of the sample in an oxidic state, after the first sputter cycle it is present in oxidic as well as in metallic form, and after the second sputter cycle solely prevailing in metallic form. In contrast, Fig. 4b)

indicates that oxidic Mg and Al outlast the first and second sputter cycle. Only after 7 sputter cycles carried out, both elements are finally found to be exclusively present in metallic form. Another significant deviation is observable for oxygen. Already after the first etch cycles, the first depth profile reveals that the oxygen signal is vanishing and remaining zero in the following. In contrast, the standard profile shows a much slower decrease of the oxygen within the ZnMgAl layer which is followed by a rapid uptake when reaching the interface to the steel substrate (constant Fe to O ratio of ~90 to 10 at.%). For the ZnMgAl layer itself the influence of the residual gas on Mg and Al appears to be not that pronounced, which is related to the low concentrations of Al and Mg within the overwhelming amount of Zn. When considering analytics of materials with higher concentrations of Al and Mg, or when information is needed with respect to the (chemical) structure of the topmost layers (essential for adhesion or corrosion studies), it is an absolutely critical issue to follow an evaluation procedure, which best reflects the real sample structure.

4. Conclusions

4.1 In the field of surface science the issue of a detrimental oxygen accumulation has in principle been known since long and was especially studied in the context of well-defined oxidation experiments or for the growth and deposition of thin films. However, this issue was to date mostly neglected for analytical studies involving, e.g, **s**putter depth profiling. The obvious solution to the problem of oxygen uptake due to the residual gas, namely lowering of the pressure and shortening the exposure time, is not sufficient. Instead, the knowledge on the behavior of all involved elements together with a well-considered sequence for acquiring high-resolution scans are crucial points to obtain profiles with higher accuracy. Therefore, it is favorable to carry out beforehand fundamental cross-checks on reference materials to predict their behavior during analysis. This strategy was exemplified in the current study, showing that i) Zn surfaces are not subjected to any changes; ii) oxygen species adsorb on Fe and steel surfaces without indications for an oxide formation over longer time scales; iii) Cr reveals a clear uptake of oxygen while chemical changes are hardly recognizable, also for longer exposure times; iv) Al and Mg show beside adsorption processes even a rapid formation of metal oxides.

From a technical point of view the operation of potentially available cold traps or the firing of titanium sublimation pumps prior the experiments is advisable. The time which is needed to complete the sample transfers and all preparation steps prior to further surface processing steps should also be taken into account, since a significant uptake of oxygen – either solely adsorbed or already forming oxides – can be critical already after a short time. Furthermore, the fact that sample cooling to low temperatures may initiate or intensify the oxidation of metal surfaces has also to be considered, especially when easily degradable compounds are studied, where cooling normally helps to decrease the rate of degradation. Finally, the sputter guns may be operated in a very gentle mode during data acquisition in order to further prevent the adsorption of particles from the residual gas.

Acknowledgements

References

[1] D.J. OíConnor, B.A. Sexton, R.St.C. Smart, Surface Analysis Methods in Materials Science, Springer Verlag, 1992.
[2] A.W. Czanderna, T.E. Madey, C.J. Powell, Beam Effects, Surface Topography, and Depth Profiling in Surface Analysis, Academic Publishers, 2002.
[3] W. Dekeyser, L. Fiermans, G. Vanderkelen, J. Vennik, Electron emission spectroscopy, in: Proceedings of the NATO Summer Institute Held at the University of Gent, August 28 – September 7, 1972, Springer Science, 2017.
[4] M.D. Losego, Interfacing Epitaxial Oxides to Gallium Nitride, NCSU Libraries, 2008 (resolver/1840.16/3747).
[5] C.R. Brundle, T.J. Chuang, K. Wandelt, Core and valence level photoemission study of iron oxide surfaces and the oxidation of iron, Surf. Sci. 68 (1977) 459–468.
[6] T.-C. Lin, G. Seshadri, J.A. Kelber, A consistent method for quantitative XPS peak analysis of thin oxide films on clean polycrystalline iron surfaces, Appl. Surf. Sci. 119 (1997) 83–92.
[7] A.P. Grosvenor, B.A. Kobe, N.S. McIntyre, Examination of the oxidation of iron by oxygen using X-ray photoelectron spectroscopy and QUASES™, Surf. Sci. 565 (2004) 151–162.
[8] K. Volgmann, F. Voigts, W. Maus-Friedrichs, The interaction of oxygen molecules with iron films studied with MIES, UPS and XPS, Surf. Sci. 604 (2010) 906–913.
[9] K. Volgmann, F. Voigts, W. Maus-Friedrichs, The interaction of H₂O molecules with iron films studied with MIES, UPS and XPS, Surf. Sci. 606 (2012) 858–864.
[10] H.J. Steffen, Use of valence band Auger electron spectroscopy to study thin film growth: oxide and diamond-like carbon films, Thin Solid Films 253 (1994) 269–276.
[11] R. Bastasz, G.J. Thomas, Surface analysis of sputtered stainless steel, J. Nucl. Mater. 76&77 (1978) 183–187.
[12] M. Frerichs, F. Voigts, W. Maus-Friedrichs, Fundamental processes of aluminium corrosion studied under ultra high vacuum conditions, Appl. Surf. Sci. 253 (2006) 950–958.
[13] J.C. Fuggle, L.M. Watson, D.J. Fabian, X-ray photoelectron studies of the reaction of clean metals (Mg, Al Cr, Mn) with oxygen and water vapour, Surf. Sci. 49 (1975) 61–76.
[14] S.J. Splinter, N.S. McIntyre, W.N. Lennard, K. Griffiths, G. Palumbo, An AES and XPS study of the initial oxidation of polycrystalline magnesium with water vapour at room temperature, Surf. Sci. 292 (1993) 130–144.
[15] D.D. Eley, P.R. Wilkinson, Adsorption and oxide formation on aluminum films, Proc. R. Soc. London A 254 (1960) 327–342.
[16] S. Ekelund, C. Leygraf, A LEED-AES study of the oxidation of Cr(110) and Cr (100), Surf. Sci. 40 (1973) 179–199.
[17] C.H.J. Palacio, D. Mathieu, A.E.S. Landolt, XPS and EELS study of the initial oxidation of polycrystalline chromium, Surf. Sci. 182 (1987) 41–55.
[18] G. Gewinner, J.C. Peruchetti, A. Jaegle, A. Kalt, Photoemission study of the chromium(111) surface interacting with oxygen, Surf. Sci. 78 (1978) 439–458.
[19] E.E. Huber, C.T. Kirk, Work function changes due to the chemisorption of water and oxygen on aluminum, Surf. Sci. 5 (1966) 447–465.
[20] N. Kasupke, M. Henzler, Oxygen on cleaved Si(111): effects of Atomic steps and residual gases, Surf. Sci. 92 (1980) 407–416.
[21] J.A. Ramsey, Exo-electron emission from abraded metal surfaces at high and ultrahigh vacuums, J. Appl. Phys. 37 (1966) 452–453.
[22] H.H. Brongersma, M. Draxler, M. de Ridder, P. Bauer, Surface composition analysis by low-energy ion scattering, Surf. Sci. Rep. 62 (2007) 63–109.
[23] M. Arndt, J. Duchoslav, H. Itani, G. Hesser, C.K. Riener, G. Angeli, K. Preis, D. Stifter, K. Hingerl, Nanoscale analysis of surface oxides on ZnMgAl hot-dip-coated steel sheets, Anal. Bioanal. Chem. 403 (2012) 651–661.
[24] D.A. Shirley, High-resolution X-ray photoemission spectrum of the valence bands of gold, Phys. Rev. B 5 (1972) 4709–4714.
[25] Thermo Scientific, The Avantage Data System, Application Note 31005, 2017 (accessed Dec. 2016) https://tools.thermofisher.com/content/sfs/brochures/D16062~.pdf.
[26] J.F. Ziegler, J.P. Biersack, U. Littmark, The Stopping and Range of Ions in Solids, vol. 1, Pergamon, New York, 1985.
[27] J. Duchoslav, M. Arndt, T. Keppert, G. Luckeneder, D. Stifter, XPS investigation on the surface chemistry of corrosion products on ZnMgAl-coated steel, Anal. Bioanal. Chem. 405 (2013) 7133–7144.
[28] C.D. Wagner, Auger lines in X-ray photoelectron spectrometry, Anal. Chem. 44 (1972) 967–973.
[29] B.R. Strohmeier, An ESCA method for determining the oxide thickness on aluminum alloys, Surf. Interf. Anal. 15 (1990) 51–56.
[30] S. Tanuma, C.J. Powell, D.R. Penn, Calculations of electron inelastic mean free paths for 31 materials, Surf. Interf. Anal. 11 (1988) 577–589.
[31] S. Tanuma, C.J. Powell, D.R. Penn, Calculations of electron inelastic mean free paths, II. Data for 27 Elements over the 50–2000 eV Range, Surf. Interf. Anal. 17 (1991) 911–926.
[32] D. Goebl, B. Bruckner, D. Roth, C. Ahamer, P. Bauer, Low-energy ion scattering: a quantitative method? Nucl. Instrum. Meth. B 354 (2015) 3–8.
[33] T. Fauster, L. Hammer, K. Heinz, A. Schneider, Oberflächenphysik: Grundlagen und Methoden, Oldenbourg Verlag, 2013.
[34] Pfeiffer Vacuum, Vacuum Technology Know How, Pfeiffer Vacuum GmbH, 2009.

[35] G. Kastirke, Konstruktion und Aufbau einer UHV-tauglichen COLTRIMS-Kammer, master thesis, Goethe University, Frankfurt am Main, 2014.

[36] D.J. Miller, M.C. Biesinger, N.S. McIntyre, Interactions of CO_2 and CO at fractional atmosphere pressures with iron and iron oxide surfaces: one possible mechanism for surface contamination? Surf. Interf. Anal. 33 (2002) 299–305.

[37] D.Y. Murzin, Engineering Catalysis, De Gruyter Graduate, 2013.

[38] S. Hofmann, Auger- and X-Ray Photoelectron Spectroscopy in Materials Science, Springer Series in Surface Sciences, 2013.

[39] M.P. Seah, W.A. Dench, Quantitative electron spectroscopy of surfaces: a standard data base for electron inelastic mean free paths in solids, Surf. Interface Anal. 1 (1979) 2–11.

[40] P.J. Cumpson, M.P. Seah, Elastic scattering corrections in AES and XPS. II. Estimating attenuation lengths and conditions required for their valid use in overlayer/substrate experiments, Surf. Interface Anal. 25 (1997) 430–446.

[41] J. Duchoslav, R. Steinberger, M. Arndt, D. Stifter, XPS study of zinc hydroxide as a potential corrosion product of zinc: rapid X-ray induced conversion into zinc oxide, Corros. Sci. 82 (2014) 356–361.

[42] R. Steinberger, J. Duchoslav, T. Greunz, M. Arndt, D. Stifter, Investigation of the chemical stability of different Cr(VI) based compounds during regular X-ray photoelectron spectroscopy measurements, Corros. Sci. 90 (2015) 562–571.

[43] R. Steinberger, J. Walter, T. Greunz, J. Duchoslav, M. Arndt, S. Molodtsov, D.C. Meyer, D. Stifter, XPS study of the effects of long-term Ar^+ ion and Ar cluster sputtering on the chemical degradation of hydrozincite and iron oxide, Corros. Sci. 99 (2015) 66–75.

[44] E.C. Goldberg, R. Monreal, F. Flores, H.H. Brongersma, P. Bauer, New model for ion neutralization at surfaces, Surf. Sci. Lett. 440 (1999) L875–L880.

[45] M. Draxler, R. Gruber, H.H. Brongersma, P. Bauer, Velocity scaling of ion neutralization in low energy ion scattering, Phys. Rev. Lett. 89 (2002), 263201-1–263201-4.

[46] P. Kürnsteiner, R. Steinberger, D. Primetzhofer, D. Goebl, T. Wagner, Z. Druckmüllerova, P. Zeppenfeld, P. Bauer, Matrix effects in the neutralization of He ions at a metal surface containing oxygen, Surf. Sci. 609 (2013) 167–171.

[47] H. Itani, J. Duchoslav, M. Arndt, T. Steck, J. Gerdenitsch, K. Preis, W. Winkler, D. Stifter, X-ray photoelectron- and scanning Auger electron spectroscopy study of electrodeposited ZnCr coatings on steel, Anal. Bioanal. Chem. 403 (2012) 663–673.

[48] H. Krueger, S.R. Pollack, The initial oxidation of aluminum thin films at room temperature, Surf. Sci. 30 (1972) 263–279.

[49] N. Wakiya, K. Kuroyanagi, Y. Xuan, K. Shinozaki, N. Mizutani, An XPS study of the nucleation and growth behavior of an epitaxial Pb(Zr, Ti)O$_3$/MgO (100) thin film prepared by MOCVD, Thin Solid Films 372 (2000) 156–162.

[50] B. Qu, Y. Wang, W. Zhong, K. Wang, Z. Wang, Surface analysis of PbTiO$_3$ films prepared by the solgel method, J. Appl. Phys. 71 (1992) 3467–3470.

[51] L.P.H. Jeurgens, M.S. Vinodh, E.J. Mittemeijer, Initial oxide-film growth on Mg-based MgAl alloys at room temperature, Acta Mater. 56 (2008) 4621–4634.

[52] K.L. Siefering, G.L. Griffin, Chemical reactions of Zn/Cu Zn/Cu$_2$O, and Zn/CuO thin films, Surf. Sci. 207 (1989) 525–538.

[53] J.A. Rodriguez, Chemical properties of bimetallic surfaces: the reaction of O$_2$ and NO$_2$ with Zn on Ru(001), J. Phys. Chem. 97 (1993) 6509–6517.

[54] J.A. Rodriguez, J. Hrbek, Decomposition of NO2 on metal surfaces: oxidation of Ag, Zn, and Cu films, J. Vac. Sci. Technol. A 12 (1994) 2140–2144.

[55] M. Schuerz, G.H. Fleischanderl, K. Luckeneder, T. Preis, G. Haunschmied, Corrosion behaviour of Zn–Al–Mg coated steel sheet in sodium chloride-containing environment, Corros. Sci. 51 (2009) 2355–2363.

[56] R. Steinberger, J. Duchoslav, M. Arndt, D. Stifter, X-ray photoelectron spectroscopy of the effects of Ar^+ ion sputtering on the nature of some standard compounds of Zn Cr, and Fe, Corros. Sci. 82 (2014) 154–164.

[57] R. Sagl, A. Jarosik, D. Stifter, G. Angeli, The role of surface oxides on annealed high-strength steels in hot-dip galvanizing, Corros. Sci. 70 (2013) 268–275.